Efficiency Improvements for Turbo-Brayton Cryocoolers for Space

M.V. Zagarola, K.J. Cragin, R.W. Hill, J.A. McCormick

Creare LLC
Hanover, NH, 03755 USA

ABSTRACT

The thermodynamic performance of turbo-Brayton cryocoolers is predicted to first order by the efficiency of the compression and expansion processes, and the thermal effectiveness of the recuperation between the high- and low-pressure streams. Other performance factors such as recovery of expansion work (a benefit); pressure losses in tubing, fittings and components; thermal parasitics from the environment; real-gas effects; and thermal performance of heat rejection and load interface heat exchangers can have negligible impact on cryocooler performance through proper design. The key then for optimization of turbo-Brayton cryocooler performance is to optimize the performance of the compressor, turbine, and recuperator. Recuperator optimization involves maximizing the heat transfer per unit volume while maintaining low axial conduction and ability to withstand launch loads. Optimization of turbines and compressors involves optimization of the aerodynamic design of the rotating and stationary flow elements while minimizing overhead losses associated with viscous drag, rotor bypass leakage, and electromagnetic losses while not compromising reliability and lifetime. This paper presents the advances in analysis, design, and fabrication techniques for the turbomachines, in particular, that have led to milestone advances in turbo-Brayton cryocooler performance.

TURBO-BRAYTON CRYOCOOLERS

Turbo Brayton cryocoolers are known for extremely low vibration emittance; flexible integration with spacecraft and payloads; ability to cool remote and distributed loads; high efficiency and low mass at low temperatures and high capacities; and long, maintenance free lifetimes. The primary components are (1) turbomachines for the compression and expansion processes, (2) recuperative heat exchangers for internal precooling, (3) electronics for power and control of the turbomachines, and (4) interface heat exchangers that connect the cryocooler to the heat rejection system and objects to be cooled. The integration hardware for these systems is relatively simple, consisting of inter component tubing, fittings, electrical harnesses, and mounting brackets.

To date, one turbo Brayton cryocooler has been fully qualified and implemented in a space application. This was in early 2002, when a single stage turbo Brayton cryocooler was installed on the Hubble Space Telescope (HST) [1]. The cryocooler provided 7 W of cooling at 70 K, replacing the solid cryogen that had depleted on the Near Infrared Camera and Multi Object Spectrometer (NICMOS). The NICMOS Cryocooler System (NCS) returned the instrument to

Cryocoolers 21, edited by R.G. Ross, Jr., J.R. Raab and S.D. Miller

operation within one month of installation and operated without degradation in performance for over six years. This refurbishment of NICMOS was an unqualified success. On orbit operation showed that the cooler, without vibration compensation, is well below very restrictive vibration emittance requirements of the telescope, and its temperature control maintained the detectors to within less than ±0.1 K in a constantly varying thermal environment. This cooler demonstrated the features and advantages of the basic components of the turbo Brayton system in a single-point cooler configuration. Other programs have successfully demonstrated the cryocooler technology at temperatures as low as 10 K [2] and to multiple cooling stages [3].

More recently, development efforts at Creare have focused on higher-capacity applications for zero-boil-off cryogen storage [4]. Here heat loads are significant at temperatures as low as 20 K for hydrogen storage. Input powers for these cryocoolers are on the order of 1 to 2 kW, much greater than for sensor cooling applications which typically limit the cryocooler to 200 to 400 W of input power. Optimization of these high-capacity cryocoolers has focused on efficiency improvements to dramatically reduce input power, which results in decreases in overall payload mass due to smaller and lighter solar panels, heat rejection radiators, and thermal buses. This paper reviews the component performance optimization leading to lower input power.

PERFORMANCE OF THE REVERSE BRAYTON CYCLE

Figure 1 provides a cycle schematic and thermodynamic diagram for a single stage Brayton cryocooler. The working fluid for load temperatures of nominally 30 K to 120 K is single phase gaseous neon, whereas helium is used for load temperatures between 4 K to 30 K. A motor driven centrifugal compressor compresses the cycle gas from low to high pressure at the warm end of the system. The heat of compression and losses associated with the compressor are rejected at ambient temperature using an aftercooler. The high pressure flow continues from the aftercooler through a recuperator where it is precooled by the low pressure flow returning from the cold end. The flow then enters a turbine where refrigeration is produced by expansion of the cycle gas. The turbine mechanical work is converted to electrical power by an alternator and is then transferred to ambient temperature where it is utilized by the electronics to control turbine speed and refrigeration load temperature. The cycle flow continues from the turbine to the load interface heat exchanger, which can take the form of a distributed cooling network for cryogen storage applications. The continuous flow nature of the cryocooler allows the cycle gas to be transported through tubing over significant distances to the objects that require cooling with high conductance, without using secondary circulation loops or heat straps. This feature reduces system input power significantly by eliminating conductance and parasitic heat load penalties associated with cryogenic heat transport, and allows extremely flexible integration with the payload.

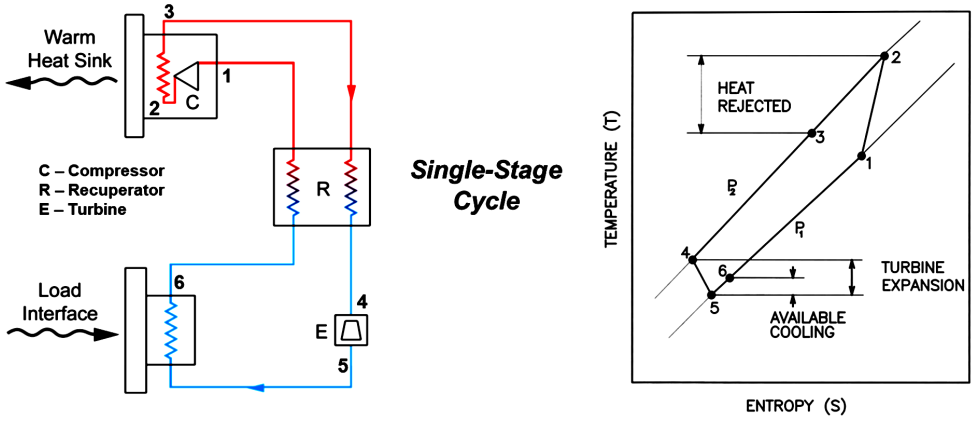

Figure 1. Single stage, reverse brayton thermodynamic cycle.

The figure of merit for a cryocooler η_{Carnot} is the cycle efficiency of the cryocooler (cooling capacity divided by input power) divided by the cycle efficiency of an ideal Carnot cycle operating at the same temperatures. That is,

$$\eta_{Carnot} = \frac{\dot{Q}_{net}}{\dot{P}_{AC,c}}\left(\frac{T_3}{T_6} - 1\right) \tag{1}$$

where $\dot{Q}_{net}$ is the net cooling load, $\dot{P}_{AC,c}$ is the AC power into the compressor, T is the cycle gas temperature, and the subscripts 3 and 6 indicate the heat rejection and cooling load state points in Fig. 1.

From the T-S diagram in Fig. 1, the net refrigeration for a turbo-Brayton cryocooler is given by:

$$Q_{net} = W_{net,t} - Q_{recup} = W_{net,t}(1 - \beta_{recuperator}) \tag{2}$$

where $\dot{W}_{net,t}$ is the turbine refrigeration and $\dot{Q}_{recup}$ is the recuperator loss given by:

$$\dot{Q}_{recup} = \dot{m}C_p(1-\varepsilon)(T_3 - T_6) \tag{3}$$

where $\dot{m}$ is the cycle mass flow rate, C_p is the specific heat of the cycle gas, and ε is the thermal effectiveness of the recuperator. In Equation 3 we have made the simplifying assumption that the cycle gas behaves as a calorically perfect gas. In addition, by using the aftercooler (T_3) and load outlet temperatures (T_6) as the heat rejection and load interface temperatures, respectively, we have assumed ideal thermal performance for these heat exchangers. These assumptions are typically consistent with turbo-Brayton cryocooler designs. Equation 2 also introduces $\beta_{recuperator}$, which is the ratio of recuperator loss to turbine refrigeration. For an ideal recuperator, $\beta_{recuperator} = 0$ and all turbine refrigeration is available as net refrigeration.

The turbine performance is characterized by its isentropic efficiency $(\eta_{turbine})$. For an isothermal turbine, where the bearings and alternator operate at nominally the same temperature as the turbine rotor, the turbine efficiency is given by:

$$\eta_{turbine} = \frac{\dot{W}_{net,t}}{\dot{W}_{s,t}} = \frac{\dot{W}_{net,t}}{\dot{m}C_pT_4\left(1 - \frac{1}{PR_t^{\frac{\gamma-1}{\gamma}}}\right)} = \eta_{aero,t}\left(1 - \frac{\dot{m}_{leak,t}}{\dot{m}}\right) - \left(\frac{\dot{W}_{drag,t} + \dot{W}_{alt,t}}{\dot{W}_{s,t}}\right) \tag{4}$$

where the subscript s represents isentropic quantities, the subscript t indicates quantities associated with the turbine, $\eta_{aero,t}$ is the aerodynamic efficiency of the turbine (actual expansion power divided by isentropic expansion power), $\dot{m}_{leak,t}$ is the flow rate of the cycle gas that bypasses the turbine rotor flow passages, and $\dot{W}_{drag,t}$ and $\dot{W}_{alt,t}$ are the turbine drag and alternator losses, respectively.

Similar to the turbine, the performance of the compressor is characterized by its isentropic efficiency $(\eta_{compressor})$:

$$\eta_{compressor} = \frac{\dot{W}_{s,c}}{\dot{P}_{AC,c}} = \frac{\dot{m}C_pT_1\left(PR_c^{\frac{\gamma-1}{\gamma}} - 1\right)}{\dot{P}_{AC,c}} = \frac{\eta_{aero,c}\left(1 - \frac{\dot{m}_{leak,c}}{\dot{m}}\right)}{1 + \eta_{aero,c}\left(1 - \frac{\dot{m}_{leak,c}}{\dot{m}}\right)\left(\frac{\dot{W}_{drag,c} + \dot{W}_{motor,c}}{\dot{W}_{s,c}}\right)} \tag{5}$$

where the subscript c indicates quantities associated with the compressor, $\eta_{aero,c}$ is the ratio of isentropic to actual compression power, and $\dot{W}_{motor,c}$ is the motor loss.

For cryocoolers with relatively high-effectiveness recuperators and low pressure drop, Equation 1 can be written in terms of component performance parameters as:

$$\eta_{Carnot} \approx \eta_{compressor}\eta_{turbine}(1-\beta_{recuperator})\frac{1}{PR^{\frac{\gamma-1}{\gamma}}}\left(1-\frac{T_6}{T_3}\right) \quad (6)$$

The impact of non-ideal performance of the recuperator, turbine, and compressor is evident from inspection of Equation 6. The compression and expansion processes are ideally isentropic with efficiencies equal to 1. Inefficiencies and losses in the compressor increase the AC input power required to produce a given pressure ratio. Inefficiencies and losses in the turbine and alternator reduce the refrigeration produced by the turbine for a given pressure ratio. Recuperator losses debit the turbine refrigeration, reducing the cooling available.

RECUPERATOR OPTIMIZATION

Recuperator optimization involves maximizing the heat transfer per unit volume while maintaining low axial conduction and ability to withstand launch loads. The legacy slotted plate recuperator flown in the NCS cryocooler utilized copper slotted plates with stainless-steel spacers and shell to reduce axial conduction. This recuperator achieved good performance with a $\beta_{recuperator}$ of 0.33. Efforts at Creare since that time have been focused on performance improvements at temperatures below 70 K and reduced recuperator size, weight, and cost at higher capacities than the NCS cryocooler. For the low temperature regime, Creare developed a silicon slotted plate recuperator that takes advantage of the extremely high conductivity of silicon at temperatures below 70 K and its low density to produce a lightweight, low-temperature recuperator [5]. Creare also developed a micro-tube recuperator that is being utilized in high-capacity turbo-Brayton cryocoolers [6] and also as the upper stage recuperator of two-stage low temperature cryocoolers [7]. In general, recuperator performance has been dictated by a trade study that considers cryocooler size, weight, power, and cost with $\beta_{recuperator}$ optimizing between 0.20 and 0.40.

TURBOMACHINE OPTIMIZATION

Performance improvements for the turbines and compressors involve optimization of the aerodynamic design of the rotating and stationary flow elements while minimizing overhead losses associated with viscous drag, leakage, and electromagnetic losses while not compromising reliability and lifetime. Minimizing overhead losses starts with selecting the proper rotor size for a given power level. Larger than optimal rotor sizes result in higher drag losses due to excessive rotor surface area and higher leakage losses due to larger diameter clearance seals. Smaller than optimal rotor sizes result in higher electromagnetic losses due to inadequate current carrying capacity of the motor/alternator coils. In addition, motor technology (e.g., permanent magnet motor versus induction motor) plays an important role in overall performance with permanent magnet motors having a clear advantage in efficiency.

To obtain improvements in aerodynamic efficiency, computational fluid dynamics (CFD) and advances in rotor fabrication techniques have been implemented concurrently at Creare. Rotor fabrication techniques utilize 5-axis CNC milling operations to faithfully produce blade geometries that are designed through CFD [8]. Legacy rotors at Creare used a line-of-sight wire EDM technique to produce the precision flow passages in the rotor, which resulted in geometric constraints that were often accompanied with compromises in performance. As an example, a CAD model of the aerodynamic design of a typical turbine rotor is shown in Fig. 2. The geometry was analyzed using ANSYS CFX. The design of the inlet nozzles, rotor, and exit diffuser were iterated within

Figure 2. Advanced turbine rotor design with shroud removed to illustrate blade design.

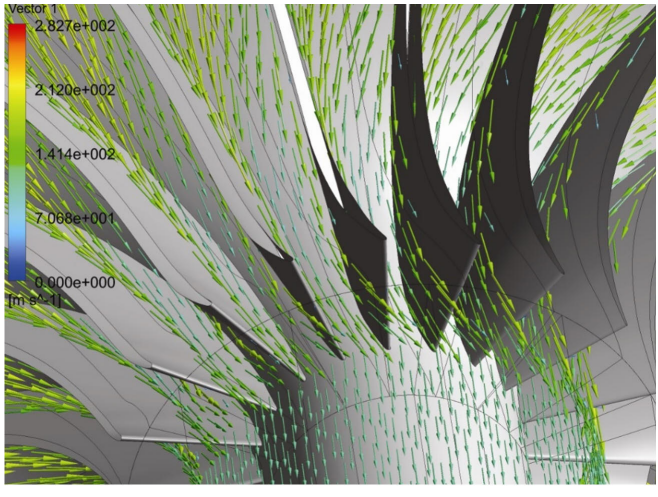

Figure 3. Velocity vectors at the turbine rotor exit illustrate removal of swirl due to proper choice of blade exit angle.

ANSYS CFX to minimize losses. For example, to minimize losses at the rotor exit, the blade contour at the exit eye was designed to remove as much swirl as possible, resulting in a pure axial flow entering the conical diffuser (see Fig. 3). Figure 4 shows the variation of the fluid entropy along the turbomachine gas path, indicating where losses occur as entropy rises.

A continuous focus on performance optimization of the turbomachines has resulted in significant improvements. For example, the first miniature, gas-bearing compressor developed by Creare was in the early 1990s. It shares the same design and served as the engineering model for the compressor in the NICMOS cryocooler. This legacy compressor utilizes an induction motor, spreadsheet optimization of aerodynamic performance, and line-of-sight rotor fabrication techniques. It has a rotor tip diameter of 0.60 in. (15 mm), operates at 7500 rev/s, and achieved a compressor efficiency of 35% at a power level of 300 W.

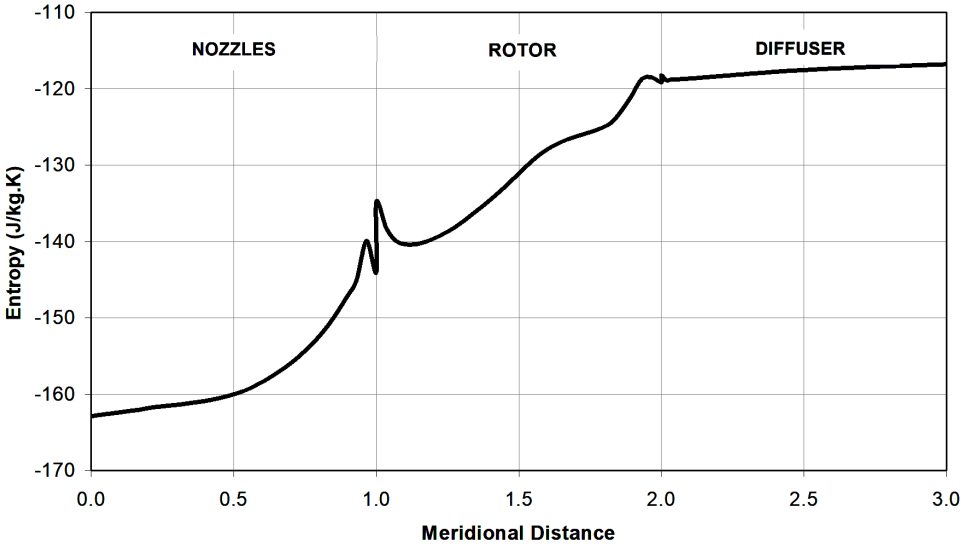

Figure 4. Entropy variation from turbine inlet to outlet is used to identify areas of high loss and optimize the design.

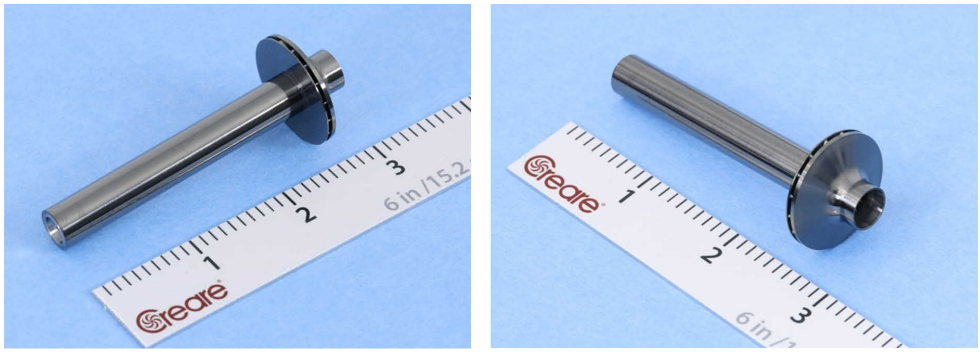

Figure 5. 1500 W-Class compressor rotor.

In comparison, our most recent compressor built for a 90 K, 150 W cryocooler on NASA Contract No. NNX17CM07C utilizes a permanent magnet motor, CFD optimization of the aerodynamic design, and advanced rotor fabrication techniques. This recent compressor rotor is shown in Fig. 5. It has a rotor tip diameter of 1.02 in. (26 mm) and operates at 4100 rev/s. The measured peak compressor efficiency is 79% at a power level of 1600 W. This represents the highest efficiency compressor built by Creare to date. The compressor test results are shown in Fig. 6.

IMPACT ON CRYOCOOLER PERFORMANCE

Improvements to turbomachine analysis and fabrication techniques since the 1990s have resulted in compressor efficiency improvements of better than 2x. Similarly, turbine efficiency improvements of slightly less than 2x have also been demonstrated. The exact value of improvement depends on power level. Nevertheless, these turbomachine efficiency improvements result in increases in Carnot efficiency for turbo-Brayton cryocoolers of 4x as deduced from Equation 7 for the same operating temperatures and pressure ratio. For a turbo-Brayton cooler operating in the 70 to 120 K temperature range, efficiencies of near 30% of the Carnot cycle are now possible, a 4x improvement in comparison to the NCS cryocooler.

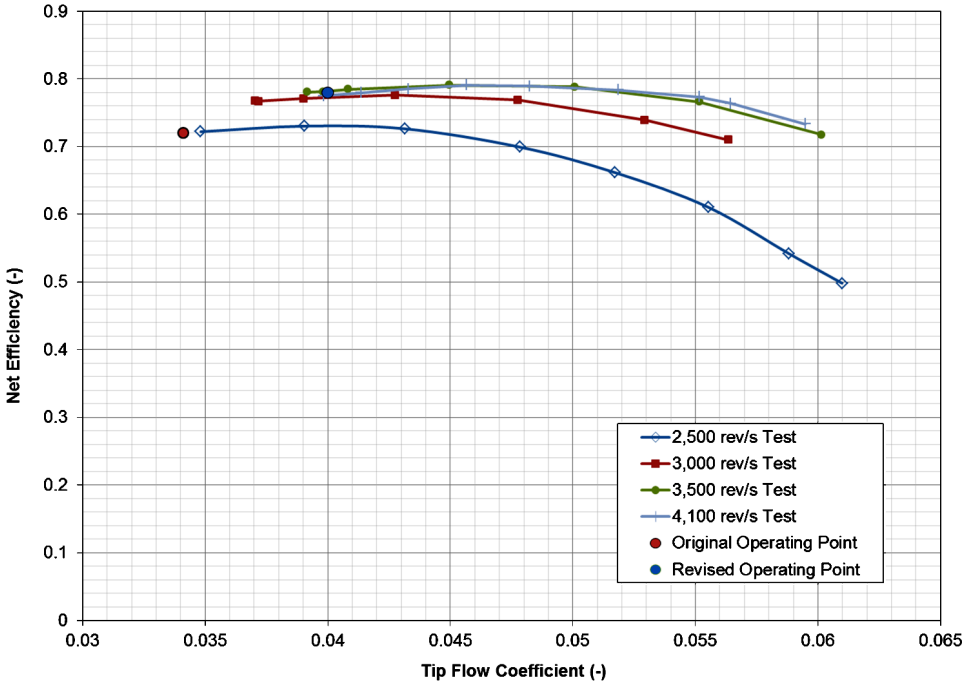

Figure 6. Compressor efficiency vs. flow coefficient.

SUMMARY

Advancements in design, analysis, and fabrication technology for turbomachine performance and recuperator size and weight over the past 30 years have enabled landmark improvements in turbo-Brayton cryocooler performance. Cryocoolers developed in the 1990s by Creare achieved efficiencies of less than 10% of the Carnot cycle and were primarily selected for missions where extremely low vibration was a driving requirement for cryocooler selection. Current component technology results in turbo-Brayton cryocoolers achieving up to 30% of the Carnot cycle at 70 to 120 K while still maintaining the inherent benefits of the technology including extremely low vibration emittance; flexible integration with spacecraft and payloads; ability to cool remote and distributed loads; high efficiency and low mass at low temperatures and high capacities; and long, maintenance free lifetimes.

ACKNOWLEDGMENTS

The authors gratefully acknowledge the support of NASA and DoD for the work presented in this paper.

REFERENCES

1. Swift, W. L., Dolan, F. X. and Zagarola, M. V., "The NICMOS Cooling System—5 Years of Successful On-Orbit Operation," *Trans of the Cryogenic Engineering Conference*, (Chattanooga, TN), edited by J. G. Weisend, II., Vol. 53, CEC, 2008, pp. 799-806.

2. Breedlove, J. J., Cragin, K. J. and Zagarola, M. V., "Testing of a Two-Stage 10 K Turbo-Brayton Cryocooler for Space Applications," *Cryocoolers 18*, edited by S.D. Miller and R.G. Ross, Jr., ICC Press, Boulder, CO (2014), pp. 445–452.

3. Zagarola, M. V., Breedlove, J. J., Kirkconnell, C. S., Russo, J. T. and Chiang, T., "Demonstration of a Two-Stage Turbo-Brayton Cryocooler for Space Applications," *Cryocoolers 15*, edited by S.D. Miller and R.G. Ross, Jr., ICC Press, Boulder, CO (2009), pp. 461–469.

4. Deserranno, D., Zagarola, M. V., Li, X. and Mustafi, S., "Optimization of a Brayton Cryocooler for ZBO Liquid Hydrogen Storage in Space," *Cryogenics*, Vol. 64, 2014, pp. 172–181.

5. Hill, R. W., Izenson, M. G., Chen, W. and Zagarola, M., "A Recuperative Heat Exchanger for Space Borne Turbo-Brayton Cryocoolers," *Cryocoolers 14*, edited by S.D. Miller and R.G. Ross, Jr., ICC Press, Boulder, CO (2007), pp. 525-533.

6. Deserranno, D., Zagarola, M. V., Craig, D., Garehan, R., Giglio, T., Smith, J., Sanders, J. K. and Day, M., "Performance Testing of a High Effectiveness Recuperator for High Capacity Turbo-Brayton Cryocoolers," *Cryocoolers 19*, edited by S.D. Miller and R.G. Ross, Jr., ICC Press, Boulder, CO (2016), pp. 447-454.

7. Niblock, A., Cragin, K., and Zagarola, M., "High Effectiveness Micro Tube Recuperators for Low Capacity Turbo Brayton Cryocoolers for Space," *Cryocoolers 21*, edited by R.G. Ross, Jr., J. Raab and S.D. Miller, ICC Press, Boulder, CO (2021), (this proceedings).

8. Hill, R. W., Hilderbrand, J. K. and Zagarola, M. V., "An Advanced Compressor for Turbo Brayton Cryocoolers," *Cryocoolers 16*, edited by S.D. Miller and R.G. Ross, Jr., ICC Press, Boulder, CO (2011), pp. 391-396.